A SMOOTH-TURN MOBILITY MODEL FOR AIRBORNE NETWORKS

Dayin He

Thesis Prepared for the Degree of

MASTER OF SCIENCE

UNIVERSITY OF NORTH TEXAS

August 2012

APPROVED:

Yan Huang, Major Professor
Yan Wan, Major Professor
Shengli Fu, Committee Member
Barrett Bryant, Chair of the Department of Computer Science and Engineering
Costas Tsatsoulis, Dean of the College of Engineering
Mark Wardell, Dean of the Toulouse Graduate School

He, Dayin. A Smooth-Turn Mobility Model for Airborne Networks. Master of Science (Computer Science), August 2012, 36 pp., 8 illustrations, references, 35 titles.

In this article, I introduce a novel airborne network mobility model, called the Smooth Turn Mobility Model, that captures the correlation of acceleration for airborne vehicles across time and spatial coordinates. Effective routing in airborne networks (ANs) relies on suitable mobility models that capture the random movement pattern of airborne vehicles. As airborne vehicles cannot make sharp turns as easily as ground vehicles do, the widely used mobility models for Mobile Ad Hoc Networks such as Random Waypoint and Random Direction models fail. Our model is realistic in capturing the tendency of airborne vehicles toward making straight trajectory and smooth turns with large radius, and whereas is simple enough for tractable connectivity analysis and routing design.

ACKNOWLEDGMENTS

Foremost, I would like to express my sincere gratitude to my advisor Dr. Yan Wan for her continuous support of my study and research, for her patience, motivation, enthusiasm and immense knowledge. Her guidance helped me in all the time of research and writing of this thesis. I could not have imagined having a better advisor and mentor for my graduate study.

I would like to thank my advisor Dr. Yan Huang and my thesis committee member Dr. Shengli Fu. Moreover, I would like to thank Dr. Fu and Dr. Kamesh Namuduri for their help to complete the thesis.

I thank my fellow labmate Yi Zhou for the stimulating discussions and for the time and effort he spent in the research work related to my thesis. Also I thank my friends in University of North Texas: Liang Xue, Thomas Ho, Ricky Chiu, Geng Zheng and Qian Wang for giving me so many good memories in Denton.

Last but not the least, I would like to thank my family: my parents Tongsheng He and Yajun Cui, for giving birth to me at the f rst place and supporting me spiritually throughout my life.

CONTENTS

CHAPTER 1

INTRODUCTION

1.1. Background of Mobility Models

The vast military and civilian applications of airborne networking have fostered dramatically growing research efforts on airborne networks (ANs) over the years. Bolstered by the advances in sensing and wireless communication technologies, ANs hold promise in providing effective, wide-applicable, low-cost, and secure information exchange among airborne vehicles. For instance, the in-flight communication among commercial airlines can allow the sharing of adverse weather conditions and emergency situations, which are of significant value especially when the flights are in areas outside the reach of ground controls. Similarly, unmanned airborne vehicles may rely on reliable communication and networking schemes for safe maneuvering. It is anticipated that ANs will be the platform of information exchange among airborne vehicles and connect with space and ground networks to complete the multiple-domain communication network in the future [29].

In the study of ANs, significant efforts have been focused on the development of routing protocols to minimize information package loss caused by link and path failures [29]. Designing robust routing strategies is challenging due to the attributes of ANs such as high node mobility and frequent topology changes. To give an example, the widely-used shortest-path routing algorithm tends to find the path with relay nodes at the edges of transmission radius [20]. As such, even a slight movement of such nodes can lead to link breakage and ultimately to path breakage. The so-called "edge effect" is particularly eminent in highly varying networks such as ANs. Therefore, we anticipate that designing reliable routing plans with reduced edge effects should rely upon the knowledge of the statistical varying structure of ANs, such as the movement pattern of AN nodes, the spatial distribution of them, and the network connectivity [8].

Mobility models commonly serve as the fundamental mathematical frameworks for network connectivity studies, network performance evaluation, and eventually the design of reliable routing protocols [12]. In particular, mobility models capture the random movement pattern of

each network agent, based on which rich information related to the varying network structure can be derived, such as node distribution and the statistics of link and path lifetime. Some mobility models have received extensive studies in the literature. The most well-known models are random direction (RD), and random waypoint (RWP) [4, 35, 7, 17]. The RWP model assumes that an agent chooses a random destination (waypoint) and traveling speed; upon the arrival, it pauses before traveling to the next destination. RD models assume that nodes travel between endpoints located at region boundaries [16]. The extended version of the RD model assumes that an agent randomly chooses a speed and direction after the completion of a randomly selected traveling time [14, 13]. The stochastic properties of these common models such as their spatial distributions can be found in e.g., [4, 24, 17, 7].

Developing suitable mobility models for ANs is no doubt the foundation for the design of realistic networking strategies among airborne vehicles. I note that the widely-used RWP and RD models are well suited to describe the random activity of mobile nodes in mobile ad hoc networks (MANETs); however, they lack the capability to describe certain features specif c to airborne vehicles. In particular, mobile nodes on ground can easily slow down, make sharp turns, and travel in an opposite direction (see an enhanced random mobility model that captures such movement [2]). However, airborne vehicles tend to maintain the same heading speed and change direction through making turns with a large radius. This unique feature is caused by the mechanical and aerodynamical constraints for airborne vehicles and ref ected in the correlation in acceleration along spatial and temporal dimensions. My aim here is to develop realistic models that capture such features unique to airborne networks, yet simple and tractable enough to facilitate connectivity analysis and routing design.

1.2. AN Mobility Models

It is worthwhile to connect our modeling efforts with the very limited existing AN mobility models [29, 32, 27]. I believe that AN mobility models need to be application-specif c, due to the wide range of variability in their applications, and different movement patterns associated with each application. Under this umbrella, let us summarize the three types of AN models in the literature including our proposed model, by focusing on: 1) the specif c application for each

model, and 2) the movement pattern associated with each. It is also worthwhile to note that these three categories of AN mobility models are associated with different levels of randomness, which I rigorously formulate and discuss in details in Chapter 4.

1) Semi-random circular movement (SRCM) mobility model for search and rescue applications. In this model, an unmanned airborne vehicle (UAV) moves around a fixed center with a randomly selected radius; after it completes a round, it chooses another radius and circles around the same center [32]. Although this model seems to be limited as the coverage is constrained by the location of the fixed circling center, I envision that it captures very well the mobility of UAVs in the search and rescue application. In search and rescue, some prior knowledge about the potential location of the search target is usually available, and UAVs are dispatched to pinpoint the exact location of the target of interest. As such, it is reasonable to use the potential target location as the fixed center in the SRCM model, and have UAVs hover around the center. The knowledge about the potential target (or equivalently, the fixed center in the SRCM model) provides extra information for trajectory prediction and the understanding of connectivity structures in the AN.

2) Flight plan-based (FP) mobility model for cargo and transportation applications. Dramatically differently, in the flight plan-based mobility model, a mobility file is created using the pre-defined flight plan, and is then converted into a time-dependent network topology map (TDNT) for the design and update of routing protocols [29]. If the actual flight status deviates from the predescribed plan, the TDNT and the relevant routes are updated. The flight plan-based model is well suited for cargo and transportation purposes, in which the entire trajectory is usually planned in advance. Although various uncertainties such as weather events, departure delays, etc., may effect the adherence to the flight plans [31, 30], the existence of a plan allows for a very good prediction of flight trajectories and hence the varying network topology beforehand [5, 18].

3) Smooth turn (ST) mobility model for patrolling applications. Both of the above two AN mobility models assume the availability of abundant trajectory information. However, in AN applications such as patrolling, a predefined trajectory or a potential target location might not be available; instead, airborne vehicles simply swarm in certain airspace. Such flexible movement resembles the highly random RD and RWP models for MANETs. In this thesis, I present a novel

mobility model named the smooth-turn mobility model (see [34] for the publication paper) , which allows f exible trajectories while also takes into account the features unique to airborne vehicles, e.g., the preference toward smooth rather than sharp turns caused by mechanical and aerodynamic constraints. Capturing such smooth-turn features in mobility models can better represent realistic maneuvering of airborne vehicles. Also, it can signif cantly improve the capability of path estimation and connectivity analysis for ANs. This new model is realistic in capturing the random movement of airborne vehicles in favor of smooth turns, and yet analyzable for node distribution and connectivity analysis. In the preparation of this thesis, I note a newly developed paper [27] which may be also suited for patrolling applications. This paper is concerned with the use of Gaussian Markov models to capture memory-equipped movement of airborne vehicles. As I discuss in Chapter 2.2 and which was also presented in [19, 23], these models do not ref ect the the kinematics of turning objects, and therefore may not realistically capture the motion of high-speed airborne vehicles.

My thesis contributes to the existing literature on mobility models in the following aspects:

- *A novel AN mobility model that captures smooth turns.* This mobility model resembles the traditional RD model, but captures the temporal and spacial correlation specif c to airborne vehicles. The model is well suited for patrolling applications, in complementary to limited existing AN models in the literature. Also, a signif cant feature of the model is that it is simple enough to serve as the framework for not only simulation studies, but also tractable theoretical analysis.
- *The stationary analysis and preliminary connectivity study of the model.* I prove that the stationary node distribution of this ST model is uniform. The nice uniformity directly leads to a series of closed-form results for connectivity, such as the expected number of neighbors, and the transition range and number of neighbors required for connectivity [3, 33].
- *The classification and comparison of different types of AN mobility models.* I identify the need to use different mobility models for different applications, and group AN mobility models according to application categories. We also characterize each category according

to the capability of predicting future trajectories. Specif cally, we def ne the *predictability* of future trajectory based upon the concept of *entropy*, and calculate that for each mobility model. We believe that this formal analysis of predictability can help better understand the difference and applicability of AN (and more general) mobility models, and more importantly, utilize the concept of predictability for the design of smart information routing algorithms.

1.3. Overview of Thesis Content

The thesis is organized as follows. In Chapter 2, I describe the ST mobility model, and Chapter 3 presents the basic analysis of its dynamics. In Chapter 3, I investigate the stationary distribution of the model through both theoretical analysis and simulation studies. Chapter 5 contains a brief summary of existing theoretical results on basic connectivity analysis. In Chapter 4, I motivate and formulate the concept of predictability, and provide a formal comparison of our model with three mobility models in the literature in terms of predicability. In Chapter 5, multiple variants and enhanced versions of the ST mobility model are discussed/simulated. Finally, a brief conclusion and discussion about future works is provided in Chapter 6.

CHAPTER 2

SMOOTH-TURN MOBILITY MODEL

In this chapter, I first describe the basic mathematical smooth turn mobility model in Section 2.1. I then discuss the roles of model parameters, and connect the model with related models in the literature in Section 2.2. The consideration of movement at boundaries are also included.

2.1. Basic Model Description

I introduce the ST mobility model to describe the movement of airborne vehicles in highly random airborne networks. The model captures the special feature of airborne vehicles—the tight temporal and multi-dimensional correlation of speed and acceleration. Incorporating this special feature into mobility models increases the predictability of a vehicle's trajectory, which in turn, provides useful information for connectivity analysis and the design of reliable information sharing strategies for ANs.

The idea behind the ST random mobility model is simple. An airborne vehicle selects a point in the space along the line perpendicular to its heading direction and circles around it until the vehicle chooses another turning center. This perpendicularity is the key that ensures the smoothness of flight trajectories. Besides that, we assume the waiting time for the change of turning centers to be memoryless, i.e., the timing of the center change does not depend on the duration for which the UAV maintains its current center. The memoryless feature of waiting time is typically used to model the occurrence of random events, and brings in the nice features of renewable processes for a tractable analysis [25]. For instance, connectivity analysis can be taken at any time instance without prior knowledge of the duration that a vehicle has kept its current centripetal acceleration. Furthermore, since a vehicle commonly favors straight trajectory and slight turns than very sharp turns, we model the inverse length of the circle radius to be Gaussian distributed.

Now let me describe the mathematics of the ST mobility model. We use $l_x(t)$, $l_y(t)$, $v_x(t)$, $v_y(t)$, $w(t)$, and $\Phi(t)$ to describe the X coordinate, Y coordinate, velocity in X direction, velocity in Y direction, angular velocity, and the heading angle of an airborne vehicle at time t. For simplicity,

we assume that a vehicle has a constant forward speed V in a 2-D plane; therefore, the vehicle has a tangential acceleration $a_t(t)$ as 0 (see Equation (1)). This is reasonable for airborne vehicles, especially jets and gliders, as they tend to maintain the same speed in f ight and "reduce speed" through zigzagging and circling.

Furthermore, the vehicle changes its centripetal acceleration $a_n(t)$ at randomly selected time points T_0, T_1, T_2, ..., with $0 = T_0 < T_1 < T_2 < ....$ The duration for the vehicle to maintain its current centripetal acceleration $\tau(T_i) = T_{i+1} - T_i$ follows exponential distribution as motivated by its memoryless property [25]. In particular, the probability density function of τ_i is $f_{\tau_i}(\tau_i) = \lambda e^{-\lambda \tau(T_i)}$, where λ is the mean duration for a vehicle to maintain its current centripetal acceleration.

Next, I describe how the new centripetal acceleration $a_n(t)$ is selected at each time point T_i. $a_n(T_i)$ is determined by the turning radius $r(T_i)$ according to $a_n(T_i) = \frac{V^2}{r(T_i)}$ (refer to Equation (2)). The selection of $r(T_i)$ also determines the new turning center with coordinates $(c_x(T_i)), c_y(T_i))$. In particular, $r(T_i)$ is the distance between the vehicle's current location $(l_x(T_i), l_y(T_i))$ and the new turning center. It is important to note that the new turning center $(c_x(T_i)), c_y(T_i))$ resides along the line perpendicular to the heading of the vehicle at time T_i, (with heading angle denoted as $\Phi(T_i)$), to guarantee smoothness. Also of particular note, the random variable $r(T_i) \in R$ allows turns to both left and right. We assume that $r(T_i) > 0$ represents that the center is to the right of the heading direction. $\frac{1}{r(T_i)}$ is a random variable that follows normal distribution with zero mean and variance σ^2. This distribution is selected so that smooth trajectories and large-radius turns are favorable than sharp turns with small radius.

Finally, Equations (3), (4) and (5) describe the relationships between location, heading angle, velocity, and angular velocity (see [19] for a review of dynamic models for moving aerial objects). In summary, the dynamics of the basic ST mobility model during the time interval $T_i \leq t < T_{i+1}$ is shown in Equation (1)-(5). Because a vehicle keeps its centripetal acceleration for a duration of T_i before changing its centripetal acceleration, it is easy to see that during the interval $T_i \leq t < T_{i+1}$, $r(t) = r(T_i)$, $a_n(t) = a_n(T_i)$, $c_x(t) = c_x(T_i)$, $c_y(t) = c_y(T_i)$, and $\tau(t) = \tau(T_i)$. A typical

trajectory of the model is shown in Figure 2.1.

$$a_t(t) = 0 \tag{1}$$

$$a_n(t) = \frac{V^2}{r(T_i)} \tag{2}$$

$$\dot{\Phi}(t) = -w(t) = -\frac{V}{r(T_i)} \tag{3}$$

$$\dot{l_x}(t) = v_x(t) = V cos(\Phi(t)) \tag{4}$$

$$\dot{l_y}(t) = v_y(t) = V sin(\Phi(t)) \tag{5}$$

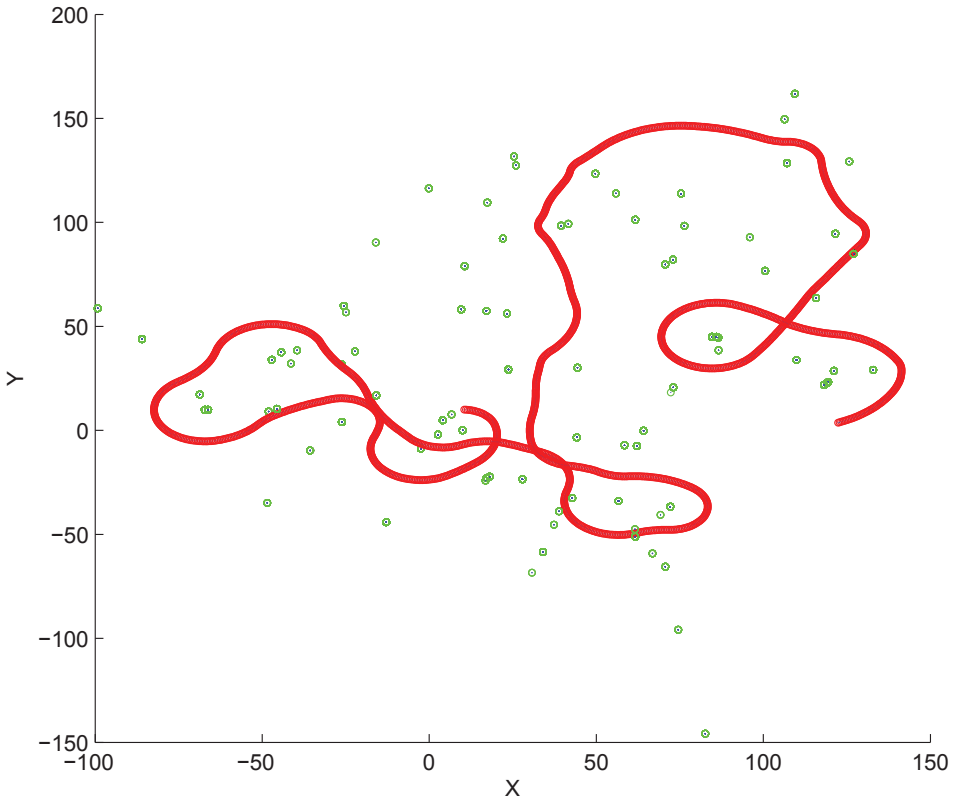

FIGURE 2.1. A simulation of the trajectory of UAV in a 2-D domain. The trajectory is shown in red. Green spots are the randomly chosen turn centers.

2.2. Further Discussions of the Model

The ST mobility model naturally captures the highly random movement patterns of ANs, and the preference toward straight trajectory or large smooth turns with constant speed. In this

section, let me first comment on the three parameters in the model, by focusing on their impacts on the mobility of ANs. I then connect the model with the RD model and the rich literature on target tracking models. Finally, I discuss two models capturing the movement at boundaries.

The first parameter is the vehicle speed V. ANs typically have high vehicle speed (in the range of $50 - 500$ miles per hour [29]), which causes highly varying connectivity structures. We keep V constant in the basic model for both simplicity and realistic considerations. I discuss enhanced models with varying V in Chapter 5. The second parameter is the mean of the exponential random variable T_i, λ. A small λ indicates that the airborne vehicle changes its turning center frequently. This results in a more wavy trajectory. The last parameter is the variance of the Gaussian variable $\frac{1}{r(T_i)}$, σ^2. σ^2 determines the preference between straight trajectory versus turns. In particular, a small variance denotes a high possibility of very large turning radius, and therefore a more straight trajectory. At the extreme, if the variance is close to 0, the ST mobility model has very straight trajectories, which resemble those of the RD model without direction change, as seen in Figure 2.2a. At the other extreme, a large σ^2, large V and small λ result in more curvy trajectories (Figure 2.2b). Through choosing proper combinations of the parameters V, λ, and σ^2, the model can capture a wide range of AN mobility patterns. The parameters to capture a specific AN mobility pattern can be estimated from the trajectory data.

It is worthwhile to connect my ST mobility model with two related categories of models in the literature. First, as my model is so close to the RD model, I can phrase our model as the RD model equipped with smooth trajectory. RD model chooses a random straight direction and follows that until it chooses the next direction. Similarly, my model chooses a random turning center and circles around it until it chooses the next center. We see in Chapter 4 that the node distribution of our model also resembles that of the RD model. Second, our model is built upon the abundant literature in the context of aerial target tracking (see e.g., [19] for a thorough review). Let us briefly discuss the works in this field so as to point out the theoretical foundation of our model. Early models in this field assume that the acceleration is uncorrelated in 2-D or 3-D space, and abstract acceleration in one coordinate as a Markov process (e.g., random noise passing through a linear system) [28, 15, 19]. The Gaussian-Markov model adopted in [27] is a variation of these

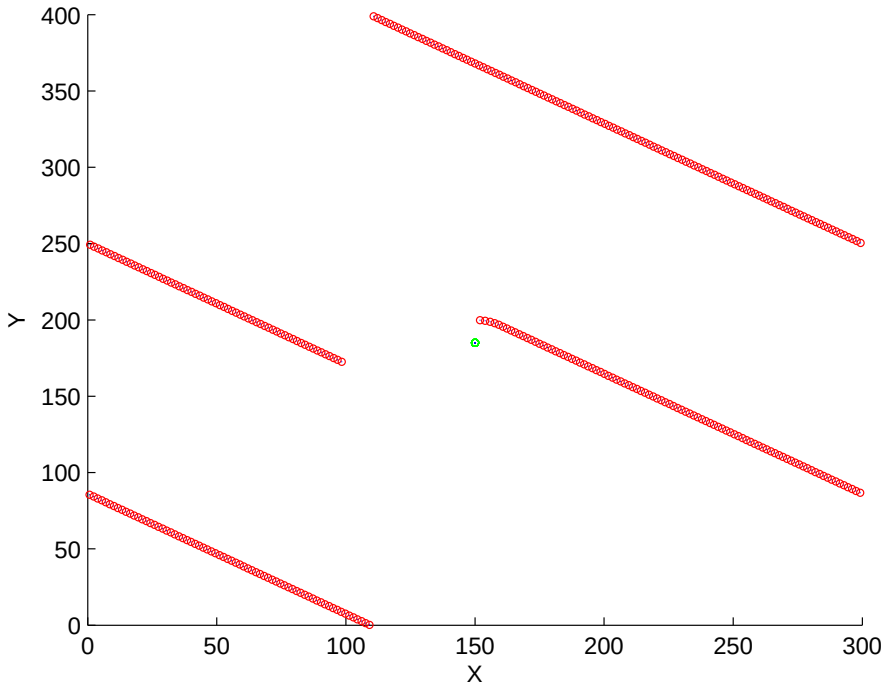

a)

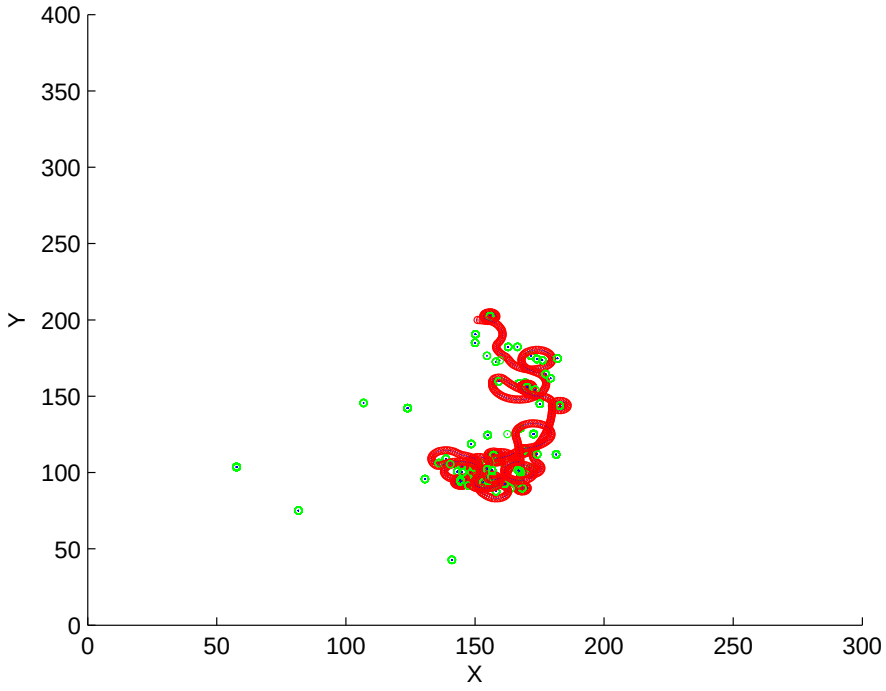

b)

FIGURE 2.2. Simulations of the smooth–turn mobility model to show the impact of parameters on the trajectories: a) when σ^2 is close to 0; b) when σ^2 is large and the ratio between V and σ^2 is large

works. The latter models, known as the coordinated turn models, reflect the physical laws of airborne objects, see e.g., [19, 23], and therefore better capture the correlation of acceleration in multiple coordinates. We stress that these latter works lay out the theoretical foundation for our ST AN mobility model, as they thoroughly studied the kinematics to reflect the correlation of motion across both temporal and spatial coordinates. However, because these models are built for target-tracking purposes, they focus on the high-precision prediction of the acceleration and paths for an individual aircraft, and therefore their motion dynamics are too complex to be directly used for our purpose. Driven by the need to model the motion of airborne vehicles at a statistical group level, we capture the correlation across spatial coordinates through a simple parameter — the radius r. Our model captures the correlation of motion across spacial and temporal coordinates very well, while is also simple enough for mobility analysis.

Another topic to discuss is the modeling of motions at boundaries. In this thesis, we adopt the boundary models typically used for the *RD* model, namely the "wrap-around" and the "reflection" models [24, 3]. In the "wrap-around" model, after an airborne vehicle hits the boundary, it wraps around and appears at the opposite side of the region. Alternatively, in the "reflection" model, the trajectory is mirrored against that boundary. Typical trajectories of these two boundary models are shown in Figure 2.3. These boundary models can capture the movement of agents in a large space [3]. Although these models generally may not appear in reality, they provide rich analyzability and permit us to focus more on the mobility itself instead of the impact of boundaries. In the rest of the thesis, we largely focus on the "wrap-around" scenario, but will also briefly discuss the "reflection" model.

2.3. Model Analysis

We consider an airborne vehicle flying within an rectangular airspace $[0,L] \times [0,W]$. Assuming the wrap-around boundary scenario, the trajectory of the airborne vehicle at time t (where $T_i \leq t < T_{i+1}$) is shown in Equation (6)-(11). These equations can be easily derived from Equations (1)-(5) by observing Figure 2.4. Of a particular note is the floor function (denoted by "$\lfloor\rfloor$") in Equation (9) which guarantees the range of $\Phi(t)$ to stay within 0 and 2π (see [24] for the detailed illustration). For the same reasoning, the floor functions in Equations (10) and (11) capture the

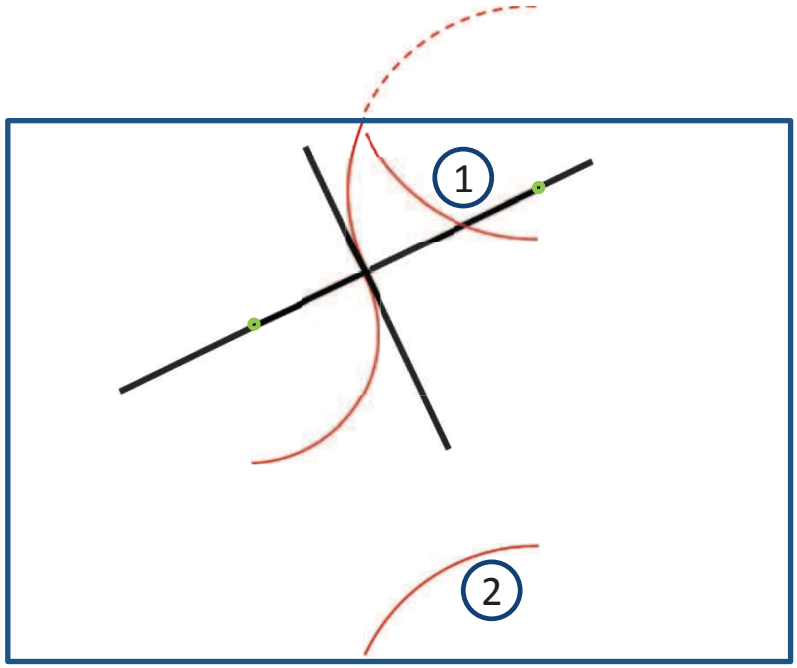

a)

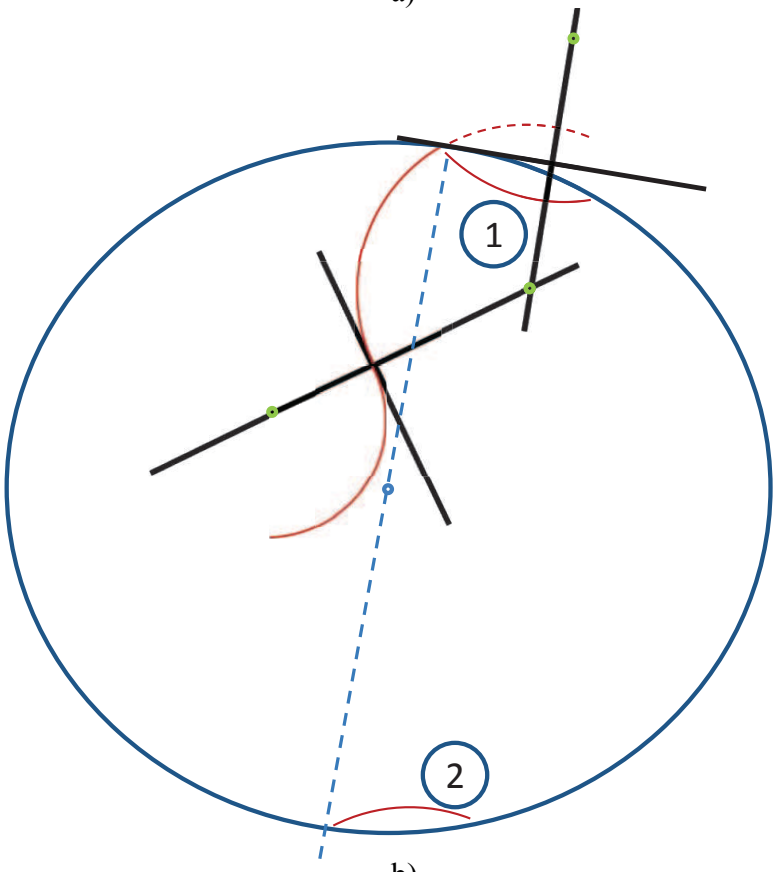

b)

FIGURE 2.3. Illustration of a) the ref ection (1) and the wrap-around (2) boundary model in a rectangular region, b) the ref ection (1) and the wrap-around (2) boundary model in a circular region.

wrap-around boundary scenario—the agent that reaches a boundary will appear at the other side of the region.

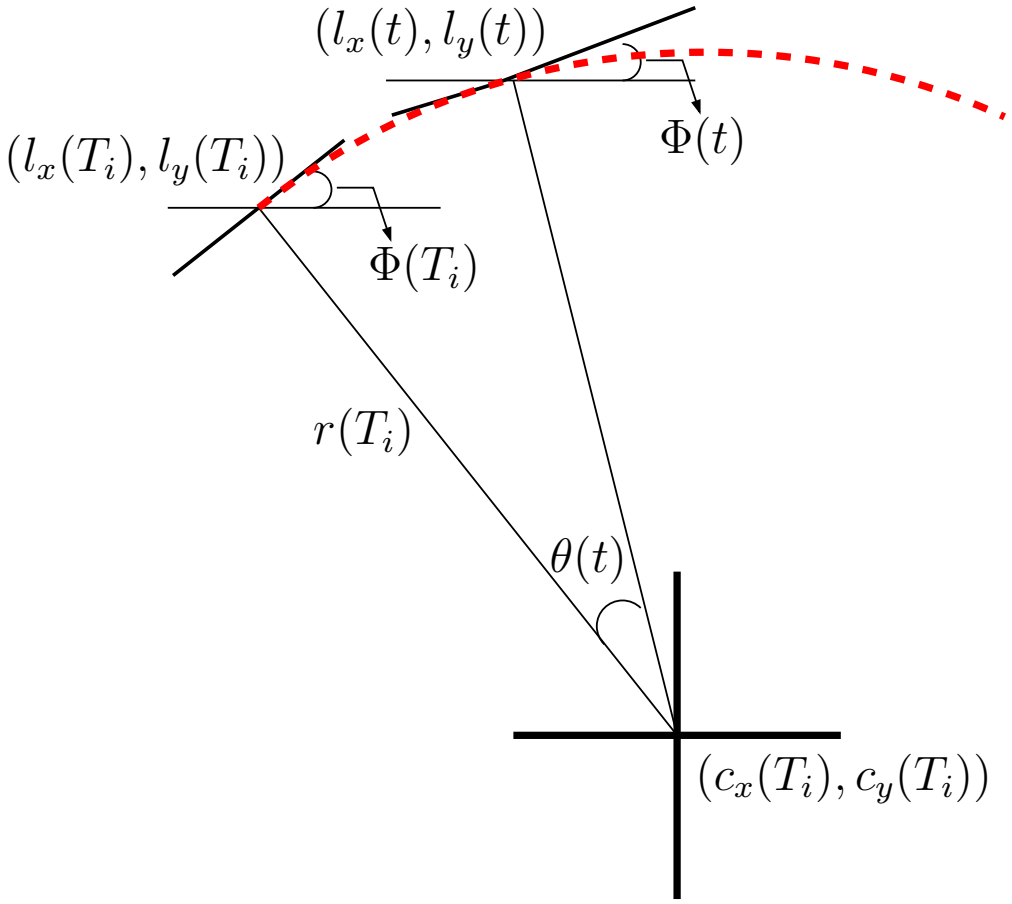

FIGURE 2.4. Trajectory analysis diagram to predict the location of an airborne vehicle at time $T_{i+1} \geq t \geq T_i$. The dashed red curve represents the trajectory of the airborne vehicle.

$$c_x(T_i) = l_x(T_i) + r(T_i)sin(\Phi(T_i)) \tag{6}$$

$$c_y(T_i) = l_y(T_i) - r(T_i)cos(\Phi(T_i)) \tag{7}$$

$$\theta(t) = \frac{V}{r(T_i)}(t - T_i) \tag{8}$$

$$\Phi(t) = \Phi(T_i) - \theta(t) - 2\pi \left\lfloor \frac{\Phi(T_i) - \theta(t)}{2\pi} \right\rfloor \tag{9}$$

$$l_x(t) = c_x(T_i) - r(T_i)sin(\Phi(t)) - W\lfloor \frac{c_x(T_i) - r(T_i)sin(\Phi(t))}{W} \rfloor \tag{10}$$

$$l_y(t) = c_y(T_i) + r(T_i)cos(\Phi(t)) - L\lfloor\frac{c_y(T_i) - r(T_i)cos(\Phi(t))}{L}\rfloor \quad (11)$$

With regard to the reflection boundary model, the only changes are to replace Equations (10) and (11) with the two following equations:

$$l_x(t) = c_x(T_i) - r(T_i)sin(\Phi(t)) - 2W\lfloor\frac{c_x(T_i) - r(T_i)sin(\Phi(t))}{2W} + 0.5\rfloor \quad (12)$$

$$l_y(t) = c_y(T_i) + r(T_i)cos(\Phi(t)) - 2L\lfloor\frac{c_y(T_i) - r(T_i)cos(\Phi(t))}{2L} + 0.5\rfloor. \quad (13)$$

The floor functions and the "+0.5" terms guarantee that the trajectory is reflected back into the region when an agent moves to the boundary (as motivated by the mathematical description of triangular wave forms). The above motion analysis results (Equations (6) to (13)) will be used to derive a variety of properties for the ST mobility model in the rest of the thesis.

CHAPTER 3

NODE DISTRIBUTION AND CONNECTIVITY

In this chapter, we consider multiple airborne vehicles in the space, f ying according to the ST mobility model. We analyze the distribution of node locations and heading angles in Chapter 3.1. These analysis is similar to that of the RD model [24], but here we also take into consideration of the smooth trajectory. The uniform distribution of node locations gives rise to interesting properties in terms of network connectivity, which we will brief y outline in section 3.2.

3.1. Node Distribution

Before presenting my results, we f rst provide the mathematical preliminary in Lemma 3.1, which will be used in the later proofs.

LEMMA 3.1. $\int_{u=0}^{b} \mathbf{1}\left\{u+a-b\lfloor\frac{u+a}{b}\rfloor < x\right\} du = x$ *holds for any* $x \in [0,b]$, *where* $a \in R$, $b \in R^{+}$, *and* $\mathbf{1}\{\}$ *is* 1 *if* $\{\}$ *is true and* 0 *if* $\{\}$ *is false.*

PROOF.

$$\int_{u=0}^{b} \mathbf{1}\left\{u+a-b\lfloor\frac{u+a}{b}\rfloor < x\right\} du = \int_{u=0}^{b} \mathbf{1}\left\{\frac{u+a}{b}-\lfloor\frac{u+a}{b}\rfloor < \frac{x}{b}\right\} du \tag{14}$$

Introducing $u' = \frac{u}{b}$, we f nd Equation (14) to be represented as

$$b\int_{u'=0}^{1} \mathbf{1}\left\{u'+\frac{a}{b}-\lfloor u'+\frac{a}{b}\rfloor < \frac{x}{b}\right\} du' = b\frac{x}{b} = x \tag{15}$$

The f rst equality holds due to the property of f oor operations [24]. □

THEOREM 3.2. *N airborne vehicles move independently in the space* $[0,L)\times[0,W)$ *according to the ST mobility model associated with wrap-around boundary model. If the initial locations of these vehicles are uniformly distributed in* $[0,L]\times[0,W]$, *and the heading angles are also initially uniformly distributed in* $[0,2\pi)$, *then the node locations and heading angles remain uniformly distributed at all times* $t > 0$.

PROOF. To prove that the mobility model maintains the uniform distribution, let us first examine a single vehicle and show that if its position and heading angle are uniformly distributed initially, they remain uniformly distributed. Then, because the airborne vehicles move independently, we can show the uniform distribution of node locations and heading angles for all vehicles.

For a moment, we consider the fixed movement pattern of a vehicle. In particular, the time sequence to change the turning center $0 = T_0 \leq T_1 \leq T_2, ...$ and the corresponding radius $r(T_0)$, $r(T_1)$, ..., are all fixed. Let us show for the particular movement pattern associated with this vehicle, uniform distribution remains for any time t.

We start with examining any time t within the duration $[T_0, T_1)$. Because the node location and heading angle are uniformly distributed at time T_0, the joint probability distribution function (pdf) of $l_x(T_0)$, $l_y(T_0)$, and $\Phi(T_0)$ can be represented as $P(l_x(T_0) < x_0, l_y(T_0) < y_0, \Phi(T_0) < \Phi_0) = \frac{x_0}{L}\frac{y_0}{W}\frac{\Phi_0}{2\pi}$, for any x_0, y_0, and Φ such at $0 \leq x_0 < L$, $0 \leq y_0 < W$, and $0 \leq \Phi < 2\pi$. In order to show that the node distributions and heading angles are uniformly distributed at at any time $T_0 \leq t < T_1$, we only need to prove that the joint pdf $P(l_x(t) < x, l_y(t) < y, \Phi(t) < \Phi) = \frac{x}{L}\frac{y}{W}\frac{\Phi}{2\pi}$ for any x, y, and Φ such at $0 \leq x < L$, $0 \leq y < W$, and $0 \leq \Phi < 2\pi$.

Equation (6) to (11) inform that $l_x(t)$, $l_y(t)$, and $\Phi(t)$ are functions of $l_x(T_0)$, $l_y(T_0)$, $\Phi(T_0)$ and $r(T_0)$, and T_0. In particular, we have

$$\Phi(t) = \Phi(T_0) - \frac{V}{r(T_0)}(t - T_0) - 2\pi \left\lfloor \frac{\Phi(T_0) - \frac{V}{r(T_0)}(t - T_0)}{2\pi} \right\rfloor \tag{16}$$

$$l_x(t) = l_x(T_0) + r(T_0)sin(\Phi(T_0)) - r(T_0)sin(\Phi(t)) - W\lfloor \frac{l_x(T_0) + r(T_0)sin(\Phi(T_0)) - r(T_0)sin(\Phi(t))}{W} \rfloor$$

$$l_y(t) = l_y(T_0) - r(T_0)cos(\Phi(T_0)) + r(T_0)cos(\Phi(t)) - L\lfloor \frac{l_y(T_0) - r(T_0)cos(\Phi(T_0)) + r(T_0)cos(\Phi(t)}{L} \rfloor.$$

For the convenience of presentation, we denote the expressions in the right of the above three equations as $\Psi(\Phi(T_0), r(T_0), t, T_0)$, $\Lambda_x(l_x(T_0), \Phi(T_0), r(T_0), t, T_0)$, and $\Lambda_y(l_y(T_0), \Phi(T_0), r(T_0), t, T_0)$, respectively. Using the abbreviated notations and according to Equation (16), we can find the joint pdf of $P(l_x(t) < x, l_y(t) < y, \Phi(t) < \Phi)$ as follows:

$$P(l_x(t) < x, l_y(t) < y, \Phi(t) < \Phi) \tag{17}$$

$$= P(\Lambda_x(l_x(T_0),\Phi(T_0),r(T_0),t,T_0) < x, \Lambda_y(l_y(T_0),\Phi(T_0),r(T_0),t,T_0) < y, \Psi(\Phi(T_0),r(T_0),t,T_0) < \Phi)$$

$$(18) \quad = \int_{\Phi(0)=0}^{2\pi} \frac{1}{2\pi} \int_{l_x(T_0)=0}^{L} \frac{1}{L} \int_{l_y(T_0)=0}^{W} \frac{1}{W} \mathbf{1}\{\Psi(\Phi(T_0),r(T_0),t,T_0) < \Phi\}$$

$$\mathbf{1}\{\Lambda_x(l_x(T_0),\Phi(T_0),r(T_0),t,T_0) < x\}\, \mathbf{1}\{\Lambda_y(l_y(T_0),\Phi(T_0),r(T_0),t,T_0) < y\}\, dxdyd\Phi(T_0),$$

$$(19) \quad = \frac{1}{2\pi WL} \int_{\Phi(0)=0}^{2\pi} \mathbf{1}\{\Psi(\Phi(T_0),r(T_0),t,T_0) < \Phi\} \int_{l_x(T_0)=0}^{W} \mathbf{1}\{\Lambda_x(l_x(T_0),\Phi(T_0),r(T_0),t,T_0) < x\}\, dx$$

$$\int_{l_y(T_0)=0}^{L} \{\Lambda_y(l_y(T_0),\Phi(T_0),r(T_0),t,T_0) < y\}\, dyd\Phi(T_0).$$

The last equality is due to the independence of the variables l_x and l_y.

According to the Lemma 3.1, we can easily see that $\int_{l_x(T_0)=0}^{W} \mathbf{1}\{\Lambda_x(l_x(T_0),\Phi(T_0),r(T_0),t,T_0) < x\}\, dx = x$. Similarly, we also have $\int_{l_y(T_0)=0}^{L} \{\Lambda_y(l_y(T_0),\Phi(T_0),r(T_0),t,T_0) < y\}\, dy = y$. As such, equation 17 can be simplif ed to

$$(20) \quad P(l_x(t) < x, l_y(t) < y, \Phi(t) < \Phi) = \frac{xy}{2\pi WL} \int_{\Phi(0)=0}^{2\pi} \mathbf{1}\{\Psi(\Phi(T_0),r(T_0),t,T_0) < \Phi\}\, d\Phi$$

$$(21) \quad = \frac{x}{L}\frac{y}{W}\frac{\Phi}{2\pi},$$

also according to Lemma 3.1. The above proof shows that the uniform distribution remains in the time interval $[T_0, T_1)$ for a particular movement pattern. Furthermore, let us denote the time right before t as t^-. We then easily observe that $\Phi(T_1) = \Phi(T_1^-)$, because choosing a new center $(c_x(T_1), c_y(T_1))$ along the line perpendicular to the heading angle $\Phi(T_1^-)$ at time T_1 does not change the heading angle of the vehicle at that particular time instance. Combined with the facts that $l_x(T_1) = l_x(T_1^-)$, $l_y(T_1) = l_y(T_1^-)$, we see that the uniform distribution also holds for the closed time interval $[T_0, T_1]$.

The proof to show that the uniform distribution remains during $[T_1, T_2]$ follows exactly the same procedure. We can then further generalize the above proof to $[T_i, T_{i+1}]$ for any $i \geq 0$. Therefore, uniform distribution remains for any time $t \geq 0$ for each particular movement pattern, and therefore generally for a particular vehicle.

Because the N airborne vehicles move independently, the jointed distribution of node locations and heading angles for these airborne vehicles is the multiplication of individual distributions.

As each individual distribution is uniform, we can conclude that the N vehicles' node locations and heading angles remain uniformly distributed at any time $t \geq 0$. The proof is complete.

□

Theorem 3.2 informs that the uniform distribution at the initial time is reserved. In the next Theorem, we present that the steady-state distribution of node location and heading angle are uniform and independent from the initial distribution.

THEOREM 3.3. *N airborne vehicles move independently in the space $[0,L]\times[0,W]$ according to the ST mobility model associated with wrap-around boundary model. Assuming that λ is finite and $\sigma \neq 0$, the distributions of node locations and heading angles are uniform in $[0,L)\times[0,W)$ and $[0,2\pi)$, respectively, in the limit of large time, regardless of the distribution at the initial time.*

PROOF. Let us first sketch the structure of the proof. We first construct a Markov process with states $S(t) = \left(l_x(t), l_y(t), \Phi(t), \frac{1}{r}(t), \tau(t)\right)$ and find the probability transition kernel for the Markov chain defined at the time sequence T_i, namely $S(T_i)$. After that, we find the invariant distribution of the Markov chain $S(T_i)$. The Palm Formula [24, 1] is then used to find the limiting probability distribution of the Markov process $S(t)$.

First, we note that $S(t)$ is a Markov process, because $S(t+\Delta t)$ is only dependent upon $S(t)$, but not on any states before time t. $S(T_i)$ for $i = 0,1,...$ form a discrete-time Markov chain. The transition probability kernel for the Markov chain $S(T_i)$ is

(22) $f(S(T_{i+1})|S(T_i)) =$

$$f(l_x(T_{i+1}) = \Lambda_x(l_x(T_i), \Phi(T_i), r(T_i), T_{i+1}, T_i), l_y(T_{i+1}) = \Lambda_y(l_y(T_i), \Phi(T_i), r(T_i), T_{i+1}, T_i),$$
$$\Phi(T_{i+1}) = \Psi(\Phi(T_i), r(T_i), T_{i+1}, T_i), \frac{1}{r}(T_{i+1}), \tau(T_{i+1})|l_x(T_i), l_y(T_i), \Phi(T_i), \frac{1}{r}(T_i), \tau(T_i))$$
$$= \mathbf{1}\{l_x(T_{i+1}) = \Lambda_x(l_x(T_i), \Phi(T_i), r(T_i), T_{i+1}, T_i)\}\mathbf{1}\{l_y(T_{i+1}) = \Lambda_y(l_y(T_i), \Phi(T_i), r(T_i), T_{i+1}, T_i)\}$$
$$\mathbf{1}\{\Phi(T_{i+1}) = \Psi(\Phi(T_i), r(T_i), T_{i+1}, T_i)\} f(\frac{1}{r}(T_{i+1}), \tau(T_{i+1})|l_x(T_i), l_y(T_i), \Phi(T_i), \frac{1}{r}(T_i), \tau(T_i)).$$

Because $\frac{1}{r}(T_i)$ and $\tau(T_i)$ are independently and identically distributed (i.i.d.) normal and

exponential random variables, we can infer that $\frac{1}{r}(T_i)$ and $\tau(T_i)$ do not dependent on $S(T_i)$. Therefore, we can simplify Equation (22) to

$$
\begin{aligned}
(23)\ & f(S(T_{i+1})|S(T_i)) \\
&= \mathbf{1}\{l_x(T_{i+1}) = \Lambda_x(l_x(T_i), \Phi(T_i), r(T_i), T_{i+1}, T_i)\}\mathbf{1}\{l_y(T_{i+1}) = \Lambda_y(l_y(T_i), \Phi(T_i), r(T_i), T_{i+1}, T_i)\} \\
&\mathbf{1}\{\Phi(T_{i+1}) = \Psi(\Phi(T_i), r(T_i), T_{i+1}, T_i) f(\frac{1}{r}(T_{i+1}), \tau(T_{i+1}))\} \\
&= \mathbf{1}\{l_x(T_{i+1}) = \Lambda_x(l_x(T_i), \Phi(T_i), r(T_i), T_{i+1}, T_i)\}\mathbf{1}\{l_y(T_{i+1}) = \Lambda_y(l_y(T_i), \Phi(T_i), r(T_i), T_{i+1}, T_i)\} \\
&\mathbf{1}\{\Phi(T_{i+1}) = \Psi(\Phi(T_i), r(T_i), T_{i+1}, T_i)\}\lambda e^{-\lambda\tau(T_{i+1})}\frac{1}{\sqrt{2\pi}\sigma}e^{-\frac{1}{2r(T_{i+1})^2\sigma^2}}
\end{aligned}
$$

The markov chain $S(T_i)$ is aperiodic, Φ-irreducible, and Harris recurrent, when $\sigma \neq 0$. Hence there exists an unique measure, which also coincides with the stationary distribution [22]. Let us prove that the invariant distribution takes the following form:

$$
(24) \qquad \lim_{i\to\infty} f(S(T_i)) = \frac{1}{L}\frac{1}{W}\frac{1}{2\pi}e^{-\lambda\tau(T_i)}\frac{1}{\sqrt{2\pi}\sigma}e^{-\frac{1}{2r(T_i)^2\sigma^2}}
$$

To prove it, we only need to show that $\lim_{i\to\infty} f(S(T_i))$ as demonstrated in Equation (24) satisf es Equation (25).

$$
(25) \qquad \lim_{i\to\infty} f(S(T_i)) = \lim_{i\to\infty} f(S(T_{i+1})) = \lim_{i\to\infty}\int_{S(T_i)\in\Omega} f(S(T_i))f(S(T_{i+1})|S(T_i))dS(T_i),
$$

where Ω represents the sample space of $S(T_i)$. The left equality is straightforward as $\tau(T_i)$ and $\tau(T_{i+1})$ are i.i.d. random variables, and $r(T_i)$ and $r(T_{i+1})$ are also i.i.d. random variables.

To show that the right side of Equation (25) holds, we substitute Equations (23) and (24) into the right side of Equation (25). Noticing that $\int_{l_x(T_i)=0}^{W}\mathbf{1}\{l_x(T_{i+1}) = \Lambda_x(l_x(T_i), \Phi(T_i), r(T_i), T_{i+1}, T_i)\}dl_x(T_i) = 1$ according to Lemma 3.1 and also similar relationships hold for $l_y(T_i)$ and $\Phi(T_i)$, we obtain

$$
\begin{aligned}
&\int_{S(T_i)\in\Omega} f(S(T_i))f(S(T_{i+1})|S(T_i))dS(T_i) = \int_{S(T_i)\in\Omega}\mathbf{1}\{l_x(T_{i+1}) = \Lambda_x(l_x(T_i), \Phi(T_i), r(T_i), T_{i+1}, T_i)\} \\
&\mathbf{1}\{l_y(T_{i+1}) = \Lambda_y(l_y(T_i), \Phi(T_i), r(T_i), T_{i+1}, T_i)\}\mathbf{1}\{\Phi(T_{i+1}) = \Psi(\Phi(T_i), r(T_i), T_{i+1}, T_i)\}\lambda e^{-\lambda\tau(T_{i+1})} \\
&\frac{1}{\sqrt{2\pi}\sigma}e^{-\frac{1}{2r(T_{i+1})^2\sigma^2}}\frac{1}{L}\frac{1}{W}\frac{1}{2\pi}e^{-\lambda\tau(T_i)}\frac{1}{\sqrt{2\pi}\sigma}e^{-\frac{1}{2r(T_i)^2\sigma^2}}d(S(T_i))
\end{aligned}
$$

$$= \frac{1}{L}\frac{1}{W}\frac{1}{2\pi}\lambda e^{-\lambda\tau(T_{i+1})}\frac{1}{\sqrt{2\pi}\sigma}e^{-\frac{1}{2r(T_{i+1})^2\sigma^2}} = f(S(T_{i+1})) \tag{26}$$

Finally, let us find the limiting probability distribution of the markov process $S(t)$. According to the Palm formula [24, 1], the limiting probability distribution of $S(t)$ can be found in the following, by conditioning upon the stationary distribution of $S(T_i)$, where $T_i \to \infty$. In particular,

$$\lim_{t\to\infty} f(S(t)) = \frac{1}{E^0[T_1]}E^0\left[\int_0^{T_1}\mathbf{1}(S(t))dt\right] \tag{27}$$

$$= \frac{1}{\lambda}E^0\left[\int_0^{T_1}\mathbf{1}(S(t))dt\right] \tag{28}$$

$$= \frac{1}{\lambda}\int_{S(T_i)\in\Omega}\int_{t=T_i}^{T_i+\tau(T_i)} f(S(T_i))f(S(t)|S(T_i))dtdS(T_i) \tag{29}$$

where E^0 represents the empirical average. As shown in Equation (28), $E^0[T_1] = \lambda$ because T_1 is independently exponentially distributed with a finite mean λ.

Furthermore, noticing that when t is between T_i and $T_i + \tau(T_i)$, $f(S(t)|S(T_i))$ can be found using Equation (23), with all T_{i+1} replaced as t. Substituting the expression of $f(S(t)|S(T_i))$ and Equation (24) into Equation (29) and using the same reasoning to derive Equation (26), we obtain

$$\begin{aligned}
&\int_{S(T_i)\in\Omega}\int_{t=T_i}^{T_i+\tau(T_i)} f(S(T_i))f(S(t)|S(T_i))dtdS(T_i) \qquad (30)\\
&= \frac{1}{L}\frac{1}{W}\frac{1}{2\pi}\lambda e^{-\lambda\tau(t)}\frac{1}{\sqrt{2\pi}\sigma}e^{-\frac{1}{2r(t)^2\sigma^2}}\int_{\tau(T_i)=0}^{\infty}\int_{t=T_i}^{T_i+\tau(T_i)}\lambda e^{-\lambda\tau(T_i)}dtd\tau(T_i)\\
&= \frac{1}{L}\frac{1}{W}\frac{1}{2\pi}\lambda e^{-\lambda\tau(t)}\frac{1}{\sqrt{2\pi}\sigma}e^{-\frac{1}{2r(t)^2\sigma^2}}\int_{\tau(T_i)=0}^{\infty}\lambda\tau(T_i)e^{-\lambda\tau(T_i)}d\tau(T_i)\\
&= \frac{1}{L}\frac{1}{W}\frac{1}{2\pi}\lambda e^{-\lambda\tau(t)}\frac{1}{\sqrt{2\pi}\sigma}e^{-\frac{1}{2r(t)^2\sigma^2}}\lambda \qquad (31)
\end{aligned}$$

Therefore, We have $lim_{t\to\infty} f(S(t)) = \frac{1}{L}\frac{1}{W}\frac{1}{2\pi}\lambda e^{-\lambda\tau(t)}\frac{1}{\sqrt{2\pi}\sigma}e^{-\frac{1}{2r(t)^2\sigma^2}}$. Integrating with respect to $\tau(t)$ and $\frac{1}{r(t)}$, we obtain that $f(l_x(t), l_y(t), \Phi(t)) = \frac{1}{L}\frac{1}{W}\frac{1}{2\pi}$ as $t \to \infty$. The proof is complete.

□

Theorems 3.2 and 3.3 demonstrate the uniform distribution of node locations and heading angles. The results also suggest the close analogy between the ST mobility model and the RD model. In particular, the smooth trajectory requirement of the ST mobility model does not change

the stationary uniform distribution, associated with the non-smooth straight trajectory in the RD model. The results can be understood, as the wrap-around model avoids the boundary impacts. A simulation of the node distribution is shown in Figure 3.2a. We note that the results also apply to the ref ection boundary model, as shown in Figure 3.2b. The proofs can be easily adapted from the proofs for Theorems 3.2 and 3.3, by noticing the equivalence between these two boundary models [24]. The results can also be applied to circular area, as shown in Figure 3.2c and 3.2d.

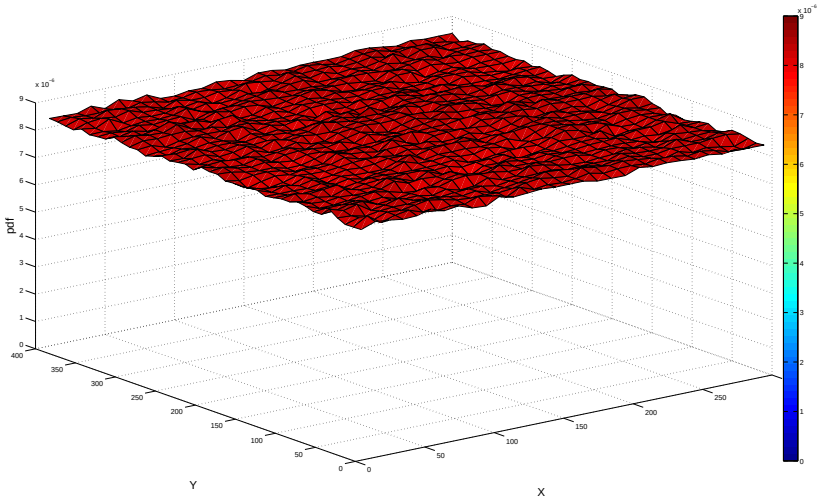

a)

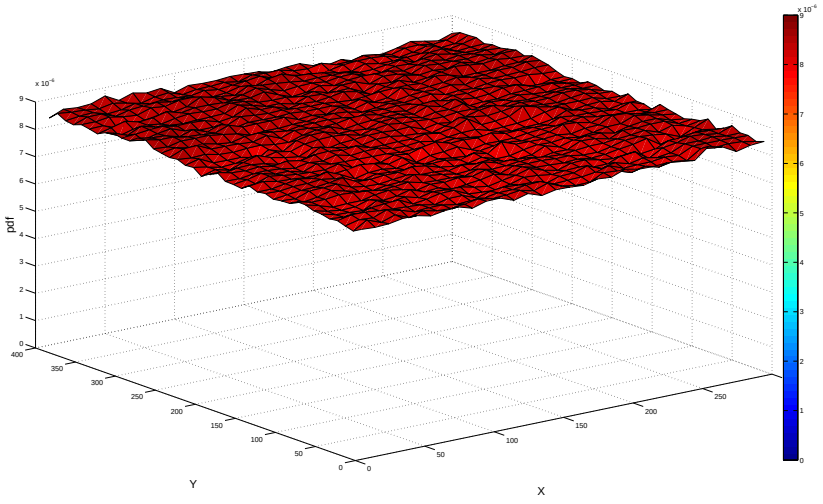

b)

FIGURE 3.1. Simulation of node distribution with: a) wrap-around model in a rectangular region, b) ref ection model in a rectangular region.

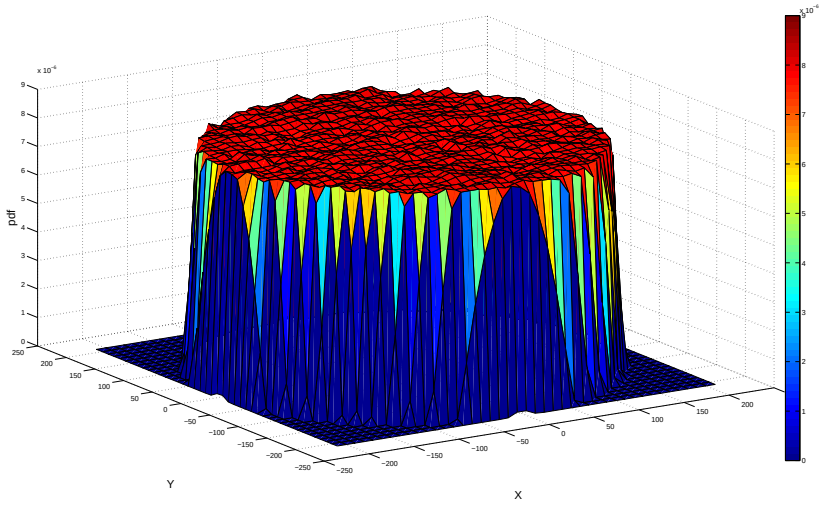

c)

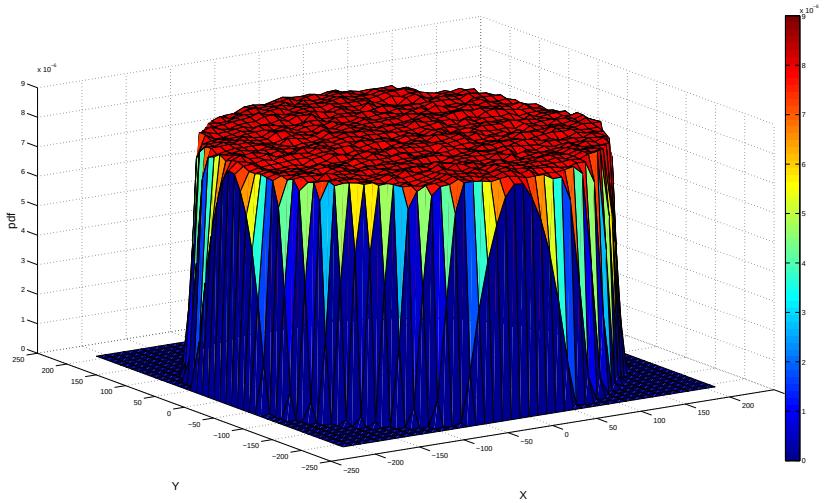

d)

FIGURE 3.2. Simulation of node distribution with: c) wrap-around model in a circular region, and d) ref ection model in a circular region.

3.2. Summary of Connectivity Properties

The uniform distribution of stationary node locations directly informs a series of results about the network's connectivity. For the completeness of our presentation, we provide a brief summary of the connectivity properties of our ST mobility model, based upon the existing connectivity studies in the literature [3, 33, 11]. For simplicity, we assume that if the distance between two airborne vehicles is within a transmission range d, the two vehicles are considered as connected [3].

3.2.1. Connectivity Properties for Individual Nodes

The number of existing neighbors for each node in a network is an important characteristic for routing algorithm design. If the expected number of neighbors is too low, the network will suffer from large transmission delay or even package drop. On the contrary, a high expected number leads to a very dense network, and thus causes problems such as harder-to-implement collision avoidance mechanisms, and the competition of limited communication channels among the agents.

For an unbounded area (i.e., simulated by the wrap-around boundary condition), the expected node degree for a given node is $E(D) = \frac{\pi N d^2}{A}$, where N is the number of nodes, and A is the area of the region [3]. For instance, for rectangular regions as shown in Theorems 3.2 and 3.3, we have $A = LW$. Furthermore, for a large n and also small d relative to A, the probability of the number of neighbors for any given node is approximately $P(D = m) = \frac{e^{-E(D)}E(D)^m}{m!}$ [3]. Therefore, the probability for a node to be isolated can be easily derived as $P(D = 0) = e^{-\frac{\pi N d^2}{A}}$ [3].

3.2.2. Connectivity Properties at a Network Level

The probability for the network to be connected, denoted as $P(connected)$, is less than or equal to the probability for the network to have no isolated nodes. The latter probability $P(No\ isolated\ Node) = (1 - P(M = 0))^N$, as demonstrated in [3]. It was also shown that $P(No\ isolated\ Node)$ is a tight bound for $P(connected)$, especially when $P(No\ isolated\ Node) \to 1$. For the wrap-around boundary model with large N with small d, this bound is approximately $e^{-Ne^{-\frac{\pi N d^2}{A}}}$ [3]. Some other studies also investigated network-level connectivity for networks with uniform distribution [11, 33]. For instance, for a circular region with boundary (e.g., the ref ection model), if the transmission range $r = \sqrt{\frac{logN + c(N)}{N\pi}}$ then $P(connected) \to 1$ as $N \to \infty$, if and only if the constant $c(N) \to \infty$.

k-connectivity is often of interest when establishing connected networks robust to agent failures. Similar to the development for 1-connectivity, the probability for the network to have no nodes with degree less than or equal to $k-1$ is a higher bound for $P(k - connected)$. In particular, $P(k - connected) \leq (1 - P(M \leq k-1))^N$. It was also shown that the higher bound is tight, especially when $P(M \leq k-1) \to 0$ [3].

CHAPTER 4

EXPLORING RANDOMNESS

I envision that the knowledge about the randomness/predictability of mobility models is a crucial factor to the design of effective routing schemes, but has not received much attention in the literature (see [2] for a brief discussion). If a mobility model captures some degree of predictability for future trajectories, routing design could be signif cantly more effective by smartly taking into account this information. At one extreme, the routing path selection for a network of agents with deterministic trajectories is fairly simple, as relative locations of agents at future times are available beforehand, and global optimization can thus be enacted to f nd the best routing design. At the other extreme, in completely random networks without any predictive information about future movement, it is highly possible that a relay node located at the boundary of transmission range (selected by the routing algorithm so as to minimize the number of hops) is moving out of the transmission range, and therefore losing data transmission. As far as our knowledge, there has not been quantitative studies on capturing the randomness/predictability for mobility models. In this Chapter, we provide an entropy measure to capture the different level of randomness among mobility models. As the focus of this thesis is on the modeling, we leave the smart utilization of this randomness/predictability information in robust routing design to the future work.

Another motivation to the study of randomness is concerned with better understanding of the AN mobility models. We observe that the three AN mobility models suitable for different applications are aligned with different levels of randomness.

For instance, mobility patterns of UAVs used for security and patrol purposes (captured by the ST mobility model) may be highly random. However, it may be more deterministic than RD model, because it captures the correlation of movement across time/space. UAVs used for search and rescue purposes (captured by the semi-circle mobility model) are usually provided with certain target location information to start with, and hence their mobility patterns are less random. Commercial aircraft and UAVs envisioned for NextGen cargo transportation have pre-planned trajectory information and hence their mobility patterns (captured by the f ight plan-based

mobility model) are almost deterministic. Because of the signif cance of mobility models in routing design, there is a need to investigate the properties of various mobility models suitable for airborne networks in great depth, and explore strategies to enhance network connectivity in each case.Randomness/predictability provides a measure for such investigation.

4.1. Def nition of Randomness/Predictability

To def ne randomness, it is natural to consider the entropy about possible future locations and directions based upon the current location and direction. We note that the entropy def ned on long look-ahead time does not help. For instance, RD, ST mobility model and the SRCM mobility model all result in uniform stationary distribution, which do not allow us to differentiate among them. Therefore, we are motivated to study immediate entropy measure at a very short time-frame, based upon the the markov chain description of the trajectory and direction dynamics.

Specif cally, we consider a markov chain, the state of which represents the status of the vehicle, including e.g., position and direction. For the convenience of presentation, we consider a discretization of time, and assume that the transition from one state to the other takes a unit time Δt, where Δt is suff ciently small. Randomness is def ned based upon the entropy rate H [10]

$$H = -\int_i \int_j p_i Q_{ij} ln Q_{ij} \tag{32}$$

where p_i is the the probability to stay at state z_i, and Q_{ij} represents the transition probability from one state i to state j.

As a special case, if the states are uniformly distributed (e.g., when $t \to \infty$ for the RD and ST mobility models) and therefore p_i are all equal, and also Q_{ij} associated with different i are the same, we can simplify Equation (32) to

$$H = -\int_j Q_{ij} ln Q_{ij} \tag{33}$$

for any i.

4.2. Comparison of Randomness for AN Mobility Models

In this section, we calculate the randomness measures for three mobility models, including RD, ST, and the f ight plan-based. The quantitative measures of randomness allow us to obtain the impact of model parameters's on the randomness performance and also compare the three different mobility models. For a fair comparison among the three mobility models, we assume that every model takes the same f xed forward speed V, all though general models may allow varying forward speed.

4.2.1. RD Mobility Model

Assume that a vehicle keeps its direction for an exponentially distributed duration (with mean λ) before choosing its new direction uniformly distributed between 0 and 2π. Because of the uniform stationary distribution of the RD model and also the memoryless property guaranteed by the exponentially distributed λ, we can use Equation (33) to obtain the randomness measure. Without loss of generality, assuming that the vehicle is moving from location 0 to the right, let us examine the probability of locations and directions at time Δt. As Δt is suff ciently small, we assume that the change of direction occurs at most once within Δt. The probability for changing direction k times follows Poisson distribution

$$P(n=k) = \frac{(\lambda\Delta t)^k e^{-\lambda\Delta t}}{k!}. \tag{34}$$

Therefore, $P(n=1) \approx \lambda\Delta t$, and $P(n=0) \approx 1-\lambda\Delta t$. If $n=0$, the vehicle moves to the right and ends up at the location $V\Delta t$ with direction to the right. If $n=1$, we assume that the change of direction occurs in the beginning, as Δ is very small. In this case, the vehicle will locate uniformly on a circle centered at the starting location with directions pointing outwards. As the direction is completely correlated with the location at Δt, we can f nd the ending location/direction with pdf $\frac{1}{2\pi}$. Therefore, we can compute the randomness as

$$\begin{aligned} H_{RD}(loc, direc) &= -P(n=0)lnP(n=0) - \int_{\Phi=0}^{2\pi} \frac{P(n=1)}{2\pi} ln \frac{P(n=1)}{2\pi} d\Phi \\ &= -(1-\lambda\Delta t)ln(1-\lambda\Delta t) - \int_{\Phi=0}^{2\pi} \frac{\lambda\Delta t}{2\pi} ln \frac{\lambda\Delta t}{2\pi} d\Phi \end{aligned} \tag{35}$$

$$= \quad -(1-\lambda\Delta t)ln(1-\lambda\Delta t) - \lambda\Delta t ln\frac{\lambda\Delta t}{2\pi}$$

Interestingly, the speed of the vehicle does not affect the randomness level of the model. Moreover, the randomness of the model increases with the increase of the parameter λ as suggested by Figure 4.1. This conclusion is reasonable, as λ represents how frequently a random direction is chosen.

4.2.2. ST Mobility Model

As def ned earlier in the thesis, we assume that a vehicle circles around for an exponentially distributed duration with mean λ, before selecting a new radius with its inverse normally distributed with mean 0 and variance σ^2. Similar to the RD case, when no change of turning center occurs within Δt, the vehicle will travel around its original turning center for a duration Δt. Otherwise, the vehicle will end up at a location with the inverse of its turning radius normally distributed. We thus can f nd randomness for the ST mobility model, in a way similar to that of the RD model, as follows:

(36)
$$\begin{aligned}
& H_{SR}(loc, direc) \\
= \quad & -P(n=0)lnP(n=0) - \int_{\frac{1}{R}=-\infty}^{\infty} \frac{P(n=1)e^{-\frac{1}{2R^2\sigma^2}}}{\sqrt{2\pi}\sigma} ln \frac{P(n=1)e^{-\frac{1}{2R^2\sigma^2}}}{\sqrt{2\pi}\sigma} d\frac{1}{R} \\
= \quad & -(1-\lambda\Delta t)ln(1-\lambda\Delta t) - \int_{\frac{1}{R}=-\infty}^{\infty} \frac{\lambda\Delta t e^{-\frac{1}{2R^2\sigma^2}}}{\sqrt{2\pi}\sigma} ln \frac{\lambda\Delta t e^{-\frac{1}{2R^2\sigma^2}}}{\sqrt{2\pi}\sigma} d\frac{1}{R} \\
= \quad & -(1-\lambda\Delta t)ln(1-\lambda\Delta t) - \lambda\Delta t ln(\lambda\Delta t) - \int_{\frac{1}{R}=-\infty}^{\infty} \frac{\lambda\Delta t e^{-\frac{1}{2R^2\sigma^2}}}{\sqrt{2\pi}\sigma} ln \frac{e^{-\frac{1}{2R^2\sigma^2}}}{\sqrt{2\pi}\sigma} d\frac{1}{R} \\
= \quad & -(1-\lambda\Delta t)ln(1-\lambda\Delta t) - \lambda\Delta t ln(\lambda\Delta t) - \lambda\Delta t(-\frac{1}{2} - ln(\sqrt{2\pi}\sigma)) \\
= \quad & -(1-\lambda\Delta t)ln(1-\lambda\Delta t) - \lambda\Delta t ln\frac{\lambda\Delta t}{\sqrt{2\pi e}\sigma}
\end{aligned}$$

The result suggests that V also does not impact the randomness of the ST mobility model. However, both λ and σ play a role in the randomness. In particular, the randomness is less with small σ, which suggests more straight trajectory. For large σ, denoting high variability of turning radius, the location and direction of the vehicle can be very uncertain. Therefore, there is a thresh-

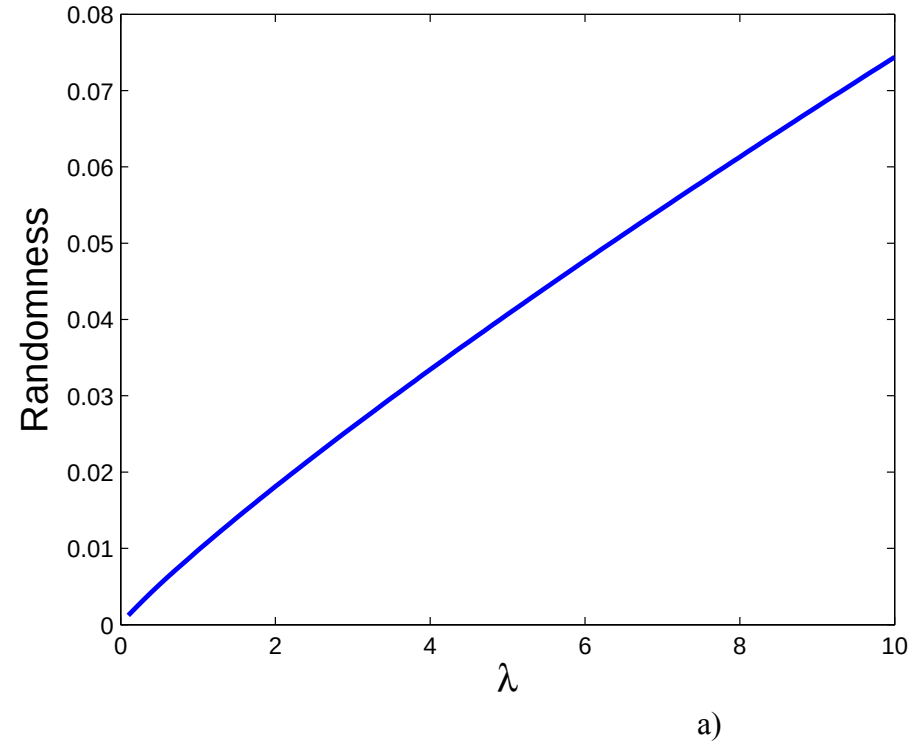

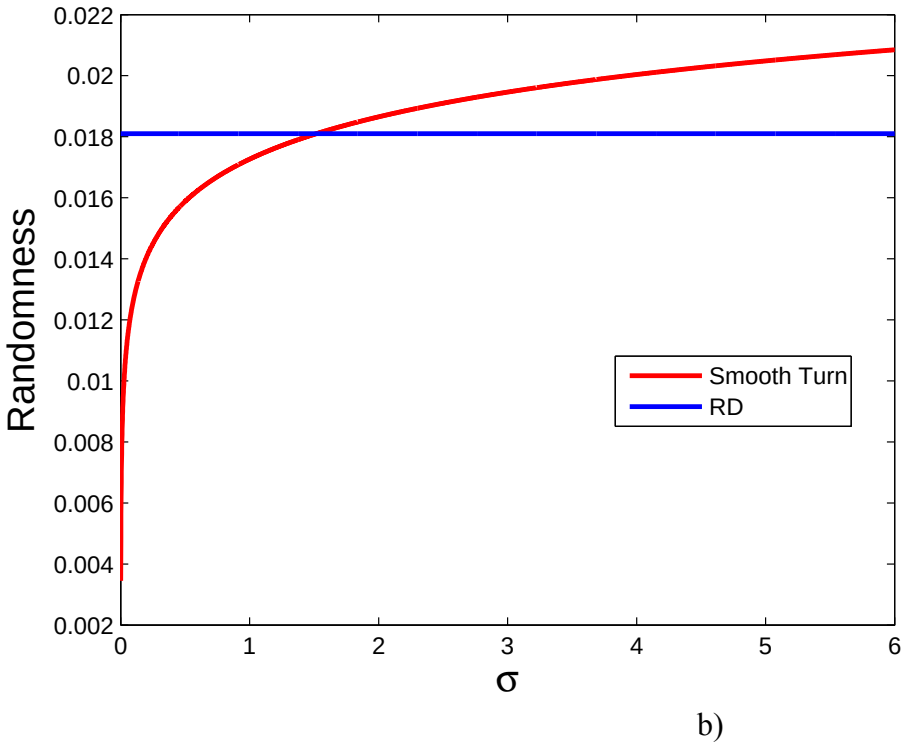

FIGURE 4.1. a) Randomness against λ in the RD model ($\Delta t = 0.001$), b) Comparison of the randomness between the RD and the ST mobility model ($\Delta t = 0.001$, $\lambda = 2$).

old for the randomness of the ST mobility model to be less than that of the RD model. Specifically, comparison of equations (36) and (37) suggests that $\sigma = \frac{2\pi}{e}$ is the threshold. A comparison of randomness for the two models can be found in Figure 4.1b.

4.2.3. Flight Plan-based Mobility Model

With the assumption that the trajectory follows the pre-planned flight path but with a tiny variation modeled by a Gaussian noise (with mean 0 and variance $\hat{\sigma}^2$), we have

$$H_{FP} = ln(\sqrt{2\pi e}\hat{\sigma}) \tag{37}$$

When $\hat{\sigma}$ is smaller than $\frac{1}{\sqrt{2\pi e}}$, the entropy is negative, representing the randomness to be less than a uniform distribution within 0 and 1 [9].

CHAPTER 5

VARIANTS OF THE ST MOBILITY MODEL

In this chapter, let us also discuss possible variants and enhancement for the ST mobility model.

5.1. Enhanced Modeling of Model Parameters

This basic ST mobility model can be easily generalized to include varying forward speed, 3D movements, etc. Airborne vehicles typically has the minimum turning radius for safety reasons. To capture this realistic issue, instead of roughly modeling $\frac{1}{r}$ as a Gaussian variable, we can provide a more detailed model for r, and require r to reside within certain safe range $[r_0, \infty]$ and $[-\infty, -r_0]$. All of the above enhancements do not change the distributions of node locations and directions. For the purpose of clear presentation, we do not include these variations in the model analysis, but realize that these new features can be easily added.

5.2. Collision Avoidance

In the current mobility model, we assume that each vehicle moves independently from each other. However, neighboring airborne vehicles need to satisfy safe separation distance, and therefore proper collision avoidance needs to be included. As collision avoidance is not the focus of this thesis, we will leave this development to the further work. However, it is worthwhile to note that as the centripetal and tangential accelerations are directly captured in the mobility model, this model has the natural capability of incorporating control mechanisms for collision avoidance (see [6] for a related implementation).

5.3. RWP-like ST Mobility Model

The current ST mobility model resembles the RD model equipped with smooth trajectory. We can similarly develop RWP-like ST mobility models. Possible strategies include: 1) randomly choosing a center which satisf es the smooth trajectory requirement and is uniformly distributed in the region, and circling around it for an exponential duration, before choosing another center; 2) randomly choosing a destination uniformly distributed in the region and reaching it through smooth

trajectory, before choosing another destination. Similar to the RWP models, we also observe the non-uniform node distributions, as shown in Figure 5.1.

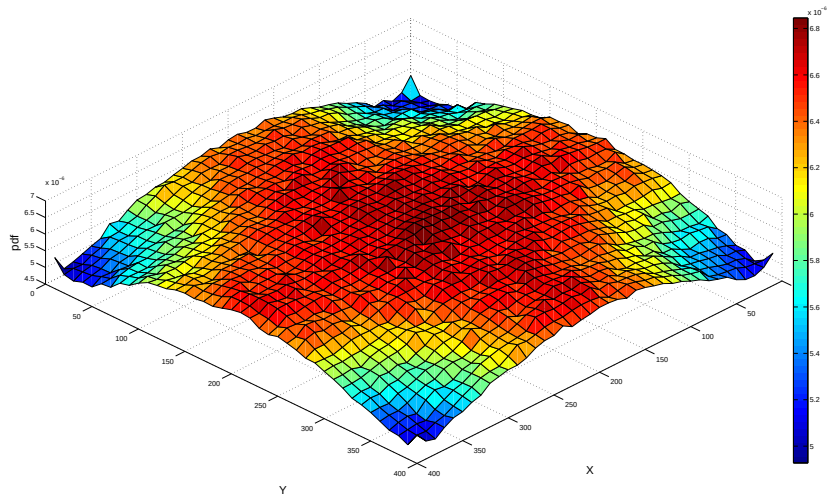

a)

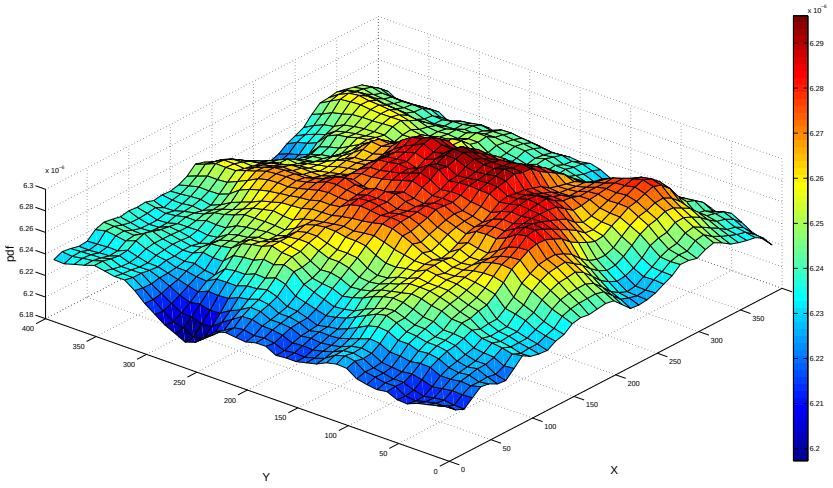

b)

FIGURE 5.1. Simulation of node distribution for a)the random-center RWP-like ST mobility model b) the random-destination RWP-like ST mobility model after smoothing.

CHAPTER 6

CONCLUDING REMARKS AND FUTURE WORKS

In this thesis, I presented a novel ST mobility for airborne networks. I prove that, similar to the RD model, the stationary node distribution is uniform. This result permits a series of analytical results on connectivity properties. I also systematically characterize randomness in mobility models. In particular, I provide a way to quantify randomness for mobility models, and use that to compare three mobility models for airborne networks. I will investigate various enhanced version of the ST mobility model as suggested in Chapter 5 in the future. I will also investigate area coverage, as whether an airborne network is able to cover the entire area of interest, and the time it takes to cover are also important characteristics for airborne networks [21, 26]. Moreover, I will further our investigation with more advanced connectivity properties such as path duration and link duration, fully investigate the impact of randomness on the performance of routing protocols, and design effective routing protocols that utilize this physical information.

BIBLIOGRAPHY

[1] F. Baccelli and P. Brémaud, *Elements of queuing theory: Palm Martingale calculus and stochastic recurrence*. Spring Verlag, 1994.

[2] C. Bettstetter, "Smooth is better than sharp: a random mobility model for simulation of wireless networks," in *ACM International Workshop on Modeling, Analysis and Simulation of Wiresless and Mobile Systems*, Rome, Italy, July 2001.

[3] C.Bettstetter, "On the connectivity of ad hoc networks," *The Computer Journal*, vol. 47, no. 4, pp. 432–447, 2004.

[4] C. Bettstetter, H. Hartenstein, and X. Pérez-Costa, "Stochastic properties of the random waypoint mobility model," *Wirelss Networks*, vol. 10, pp. 555–567, 2004.

[5] K. Bilimoria, B. Sridhar, G. Chatterji, K. Sheth, and S. Grabbe, "FACET: Future ATM concepts evaluation tool," *Air Traffic Control Quarterly*, vol. 9, no. 1, pp. 1–20, 2001.

[6] F. Borrelli, T. Keviczky, and G. J. Balas, "Collision-free uav formation f ight using decentralized optimization and invariant sets," *in Proceedings of 43rd IEEE Conference on Decision and Control*, 2004.

[7] J. Boudec and M. Vojnovic, "Perfect simulation and stationarity of a class of mobility models," Techinical Report IC/2004/59, Tech. Rep., 2004.

[8] Z. Cheng and W. B. Heinzelman, "Exploring long lifetime routing (llr) in ad hoc networks," in *Proceedings of the 7th ACM International Symposium on Modeling, Analysis and Simulation of Wireless and Mobile Systems*, 2004.

[9] K.Conrad, "Probability distributions and maximum entropy," http://www.math.uconn.edu/∼kconrad/blurbs/entropy.pdf.

[10] L. Ekroot and T. M. Cover, "The entropy of markov trajectories," *IEEE Transations on information theory*, vol. 39, no. 4, pp. 1418–1421, July 1993.

[11] N. M. Freris, H. Kowshik, and P. R. Kumar, "Fundamentals of large sensor networks: Connectivity, capacity, clocks and computation," *in Proceedings of IEEE*, vol. 98, no. 11, pp.

1828–1846, 2010.

[12] R. Ghanta and S. Suresh, "Inf uence of mobility models on the performance of routing protocols in ad-hoc wireless networks," *in Proceedings of IEEE 59th Vehicular Technology Conference*, pp. 2185–2189, 2004.

[13] B. Gloss, M. Scharf, and D. Neubauer, "A more realistic random direction mobility model," in *Proceedings of 4th Management Committee Meeting*, Würzburg, Germany, October 2005.

[14] R. A. Guérin, "Channel occupancy time distribution in a cellular radio system," *IEEE Transactions on Vehicular Technology*, vol. 35, no. 3, pp. 89–99, August 1987.

[15] J. P. Helferty, "Improved tracking of maneuvering targets: the use of turn-rate distributions for acceleration modeling," *in Proceedings of the 1994 IEEE International Conference on Multisensor Fusion and Integration for Intelligent Systems*, pp. 515–520, October 1994.

[16] D. Hong and S. S. Rappaport, "Traff c model and performance analysis for cellular mobile radio telephone systems with prioritized and nonprioritized handoff procedures," *IEEE Transactions on Vehicular Technology*, vol. 35, no. 3, pp. 77–92, August 1986.

[17] E. Hyytiä, P. Lassila, and J. Virtamo, "Spatial node distribution of the random waypoint mobility model with applications," *IEEE Transactions on mobile computing*, vol. 5, no. 6, pp. 680–694, June 2006.

[18] e. a. L. A. Wojcik, "World regional air traff c modeling with DPAT," *MITRE Technical Report MTR-97W00000070*, 1997.

[19] X. R. Li and V. P. Jilkov, "A survey of maneuvering target tracking: dynamic models," *Proceedings of SPIE Conference on Signal and Data Processing of Small Targets*, vol. AES-6, no. 4048, pp. 212–235, April 2000.

[20] G. Lim, K. Shin, S. Lee, H. Yoon, and J. Ma, "Link stability and route lifetime in ad-hoc wireless networks," in *Proceedings of International Conference on Parallel Processing*, 2002.

[21] B. Liu, O. Dousse, P. Nain, and D. Towsley, "Dynamic coverage of mobile sensor networks," *Computing Research Repository*, vol. abs/1101.0376, 2011.

[22] S. P. Meyn and R. L. Tweedie, *Markov Chains and Stochastic Stability*. Springer Verlag, 1993.

[23] N. Nabaa and R. H. Bishop, "Validation and comparison of coordinated turn aircraft maneuver models," *IEEE Transactions on aerospace and electronic systems*, vol. 36, no. 1, pp. 250–255, January 2000.

[24] P. Nain, D. Towsley, B. Liu, and Z. Liu, "Properties of random direction models," in *Proceedings of 24th Annual Joint Conference of the IEEE Computer and Communications Societies*, March 2005, pp. 1897–1907.

[25] A. Papoulis and S. U. Pillai, *Probability, random variables and stochastic processes*. McGraw-Hill, 2002.

[26] Y. Peres, A. Sinclair, P. Sousi, and A. Stauffer, "Mobile geometric graphs: Detection, coverage and percolation," *Proceedings of the Twenty-Second Annual ACM-SIAM Symposium on Discrete Algorithms*, pp. 412–428, 2011.

[27] J. P. Rohrer, E. K. Cetinkaya, H. Narra, D. Broyles, K. Peters, and J. P. G. Sterbenz, "Aerorp performance in highly-dynamic airborne networks using 3d gauss-markov mobility model," in *Proceedings of Military Communications Conference*, 2011.

[28] R. A. Singer, "Estimating optimal tracking f lter performance for manned maneuvering targets," *IEEE Trans. Aerospace and Electronic Systems*, vol. AES-6, pp. 473–383, 1970.

[29] A. Tiwari, A. Ganguli, A. Sampath, D. Anderson, B. h. Shen, N. Krishnamurthi, J. Yadegar, M. Gerla, and D. Krzysiak., "Mobility aware routing for the airborne network backbone," *in Proceedings of Military Communications Conference*, November 2008.

[30] Y. Wan and S. Roy, "A scalable methodology for evaluating and designing coordinated air traff c f ow management strategies under uncertainty," *IEEE Transactions on Intelligent Transportation Systems*, vol. 9, no. 4, pp. 644–656, 2008.

[31] Y. Wan, S. Roy, and B.Lesieutre, "Uncertainty evaluation through mapping identif cation in intensive dyna tions," in *Proceedings of AIAA Conference on Guidance, Navigation, and Control Conference and Exhibit. Extended version in IEEE Transactions on Systems, Man, and Cybernetics A, in press*, Honolulu, HI, August 2008.

[32] W. Wang, X. Guan, B. Wang, and Y. Wang, "A novel mobility model based on semi-random circular movement in mobile ad hoc networks," *Information Science*, vol. 180, pp. 399–413,

2010.

[33] F. Xue and P. R. Kumar, “The number of neighbors needed for connectivity of wireless networks,” *The Computer Journal*, vol. 10, pp. 169–181, 2004.

[34] Y. Z. D. H. Yan Wan, Kamesh Namuduri and S. Fu, “A smooth-turn mobility model for airborne networks,” *ACM Mobihoc conference*, 2012.

[35] J. Yoon, M. Liu, and B. Noble, “Sound mobility models,” *Proceedings of the Ninth Annual International conference on Mobile Computing and Networking*, pp. 205–216, 2003.